



**COMPUMAG
2009**



Florianópolis, Brazil

Proceedings of the
**17th Conference on the Computation of
Electromagnetic Fields**

November, 22nd – 26th
Florianópolis, Brazil

ORGANISATION:



SPONSORING:



PC2.12	608
Slit Effect of Laminated Stator Core in Transverse Flux Rotary Machine	
<i>Ji-Young Lee, Seung-Ryul Moon, Do-Hyun Kang, Jung-Pyo Hong</i>	
PC2.13	610
Design and Analysis of a Written-pole Motor Using a Symmetric Field and FE Methods	
<i>Byung-Taek Kim, Dae-Kyong Kim, Byung-Il Kwon</i>	
PC2.14	612
Inductance Calculation and Measurement of Interior Permanent Magnet Synchronous Motor	
<i>Tao Sun, Soon-O Kwon, Jeong-Jong Lee, Geun-Ho Lee, Jung-Pyo Hong</i>	
PC2.15	614
Shape Optimization of a Thomson-coil Actuator for Fast Response Using Topology Modification	
<i>Wei Li, Jiang Lu, Young Woo Jeong, Chang Seop Koh</i>	
PC2.16	616
Optimized Axially Magnetized Permanent Magnet Tubular Actuator: Pole-Piece Shaping	
<i>Laurentiu Encica, Johan Paulides, Koen Meessen, Bart Gysen, Jorge Duarte, Elena Lomonova</i>	
PC2.17	618
Permanent Magnet Wheel Motor for Electric Vehicle Applications	
<i>Konstantinos I. Laskaris, Anastasios G. Vichos, Antonios G. Kladas</i>	
PC2.18	620
Optimized geometrical parameters of a SRM by numerical-analytical approach	
<i>Ammar Bentounsi, Redem Rebbah, Fares Rebbahi, Hind Djeghloud, Hocine Benalla, Soltane Belakehal, Bachir Batoun</i>	
PC2.19	622
Methods for efficient computation and visualization of magnetic flux lines in 3D	
<i>Martin Hafner, Marc Schöning, Marcin Antczak, Andrzej Demenko, Kay Hameyer</i>	
PC2.20	624
Calculation of Copper Losses in Intercell Transformers by 2D FEM simulation	
<i>Bernardo Cougo, Thierry Meynard, François Forest, Eric Labouré</i>	

An Improved AC Standstill Inductance Test Method for Interior PM Synchronous Motor Considering Current Vector Variation

Tao Sun¹, Jin Hur², and Jung-Pyo Hong¹, *Senior Member, IEEE*

¹Department of Automotive Engineering, Hanyang University, Seoul, CO 133791, Korea

²School of Electrical Engineering, Ulsan University, Ulsan, CO 680749, Korea

An improved AC standstill inductance measurement method for interior permanent magnet synchronous machine (IPMSM) is proposed in this paper. Only the 3-phase voltage source, oscilloscope, and DC voltage source are required in this method, rather than the dynamometer in the other methods. Depending on the derivative q- and d-axis voltage equations in the stationary reference frame, the q- and d-axis inductances at different current magnetite and vector angle can be calculated by the measured 3-phase voltages and currents. And hence, the saturation and cross-magnetizing effect of the inductances are measurable. This paper will introduce the principle equations, experiment setup, data processing, and results comparison.

***Index Terms*—AC Standstill Method, Inductance, Cross-magnetizing Effect, Interior Permanent Magnet Synchronous Motor**

I. INTRODUCTION

Interior permanent magnet synchronous motors (IPMSM) have been widely applied in the industry and household appliances. When predict their steady-state performance during motor design, or process the vector control in the motor drive, the accuracy is strongly determined by the knowledge of the d- and q-axis inductances. Due to the saturation and cross-magnetizing effect, however, it is quite difficult to calculate and measure these inductances [1]. Several numerical methods have been proposed to solve the calculation problem [1]-[6]. The saturation, cross-magnetizing and other effect can be completely considered and calculated in these methods.

Various experiment methods also have been introduced in many literatures [2]-[5]. In [2] a method called AC standstill is introduced. This method applies an AC voltage source to one phase, and measures the currents and voltages of this phase and another phase in order to calculate the self- and mutual-inductances, and then calculate d- and q-axis inductances with them. It is called standstill because the rotor is locked at every test mechanical position. The drawbacks of this method are the effect of current vector angle varying cannot be reflected, and hence the cross-magnetizing effect is regardless. Additionally, the flux path in two-phase exciting will be different with the one of three-phase exciting. [3] proposed an improved standstill method with considering the both saturation and cross-magnetizing effect. It fixes the rotor position and uses a vector controller to generate a stepwise d- or q-axis voltage, meanwhile, keep the other axis current constant. According to the current response, the two-axis inductances can be calculated. The difficulty of this method is the generation of the stepwise voltage. In the ordinary 3-phase inverter, it cannot be directly obtained from the pulse width modulation (PWM) voltage. A high precision low-pass filter

must be used. According to phase shift between the flux linkages under the load condition and no-load condition in the steady state, [4] measured the two-axis inductances in the operation conditions. Keep one phase constant, and adjust the load torque with a dynamometer so that the total magnitude and vector angle of the load current can be covered. The inherent errors in this method are the unregarded PM demagnetization, and much varying resistance. Based on the proposed equations in [3] and [5] proposed an improved method of [4]. In this method, a look-up table is used to correct the error due to the demagnetization of the PM. However, because of the employing of the low-pass filters, the phase lag and amplitude of sensed voltage should be much careful.

As mentioned above, in order to measure the saturation and cross-magnetizing effect, the vector controller and drive have to be applied. Although the stepwise voltage generator in [3] could be used for the various-power motors, it has some special configuration. When the proper motor drive is absent, these inductance test methods such as [4] and [5] become unavailable. In addition, the expensive dynamometer is not ordinary equipment, especially for the laboratory in college. Its utilization much increases the cost of the experiment system.

Considering the practical requirements, this paper proposes a relative low cost, simple and tradeoff method. It measures the inductances in standstill condition, in order to avoid utilization of dynamometer. It uses a 3-phase low voltage AC source so that the vector controller and inverter are not required. Hence, it is very suitable for normal laboratory experiment. The most meaningful point is that this method still can consider the saturation and cross-magnetizing effect. In this paper, first, the principle of this method will be introduced. And then, based on the final equations, the experiment scheme and the processing methods of measured data will be proposed. After briefly introduce the inductance calculation method used in this paper, the experiment results will be shown and compared with the corresponding calculated results. In the final section, the drawbacks and

Manuscript received December 23, 2009

Corresponding author: Jung-Pyo Hong (e-mail: hongjp@hanyang.ac.kr)

Digital Object Identifier inserted by IEEE

errors of this method is discussed.

II. PRINCIPLE OF IMPROVED AC STANDSTILL METHOD

A. Inductances in Stationary Reference Frame

The voltage equation of the IPMSM in the stationary reference frame is described in (1) [6].

$$\begin{aligned} \begin{bmatrix} v_q^s \\ v_d^s \end{bmatrix} &= \begin{bmatrix} r_s & 0 \\ 0 & r_s \end{bmatrix} \begin{bmatrix} i_q^s \\ i_d^s \end{bmatrix} + \begin{bmatrix} p & 0 \\ 0 & p \end{bmatrix} \begin{bmatrix} \lambda_q^s \\ \lambda_d^s \end{bmatrix} \\ \begin{bmatrix} \lambda_q^s \\ \lambda_d^s \end{bmatrix} &= \begin{bmatrix} L_q^s & -L_{qd}^s \\ -L_{qd}^s & L_d^s \end{bmatrix} \begin{bmatrix} i_q^s \\ i_d^s \end{bmatrix} + \begin{bmatrix} \lambda_m \sin \theta_{er}^s \\ \lambda_m \cos \theta_{er}^s \end{bmatrix} \\ L_q^s &= L + \Delta L \cos(2\theta_{er}^s) \\ L_d^s &= L - \Delta L \cos(2\theta_{er}^s) \\ L_{qd}^s &= \Delta L \sin(2\theta_{er}^s) \end{aligned} \quad (1)$$

where r_s is the phase resistance, λ_m is the flux linkage of PM, p represents the d/dt operator, the subscript e represents the unit in electrical angle, θ_{er}^s is the rotor position in stationary reference frame, and the L and ΔL are calculated by (2).

$$\begin{aligned} L &= \frac{L_q^r + L_d^r}{2} \\ \Delta L &= \frac{L_q^r - L_d^r}{2} \end{aligned} \quad (2)$$

i.e.,

$$\begin{aligned} L_q^r &= L + \Delta L \\ L_d^r &= L - \Delta L \end{aligned} \quad (3)$$

where L_q^r and L_d^r are the desired q- and d-axis inductances in the rotation reference frame.

B. Fundamental Equations of Improve Test Method

Expand (1), and (4) is obtained.

$$\begin{aligned} v_q^s &= r_s i_q^s + \left(L + \Delta L \cos(2\theta_{er}^s) \right) \frac{d}{dt} i_q^s - 2\omega_{er}^s \Delta L \sin(2\theta_{er}^s) i_d^s \\ &\quad - \Delta L \sin(2\theta_{er}^s) \frac{d}{dt} i_d^s - 2\omega_{er}^s \Delta L \cos(2\theta_{er}^s) i_d^s + \omega_{er}^s \lambda_m \cos \theta_{er}^s \\ v_d^s &= r_s i_d^s + \left(L - \Delta L \cos(2\theta_{er}^s) \right) \frac{d}{dt} i_d^s + 2\omega_{er}^s \Delta L \sin(2\theta_{er}^s) i_q^s \\ &\quad - \Delta L \sin(2\theta_{er}^s) \frac{d}{dt} i_q^s - 2\omega_{er}^s \Delta L \cos(2\theta_{er}^s) i_q^s - \omega_{er}^s \lambda_m \sin \theta_{er}^s \end{aligned} \quad (4)$$

It is obvious that the terms with ω_{er}^s can be eliminated in the standstill condition. And in order to eliminate the sine and cosine terms, the rotor position θ_{er}^s is set to 0° (or 90°). Thus the equations are simplified as (5).

$$\begin{aligned} v_q^s &= r_s i_q^s + L_q^r \frac{d}{dt} i_q^s \\ v_d^s &= r_s i_d^s + L_d^r \frac{d}{dt} i_d^s \end{aligned} \quad (5)$$

where the v_q^s , v_d^s , i_q^s and i_d^s are the q- and d-axis voltages and currents. According to the 3-phase to 2-phase transformation in the stationary reference frame (6), they can be represented by 3-phase voltages and currents that are directly measurable

variables. In practice, (5) is modified as (7) considering the sampling data.

$$\begin{aligned} \begin{bmatrix} f_a^s \\ f_b^s \\ f_c^s \end{bmatrix} &= \frac{2}{3} \begin{bmatrix} 1 & -\frac{1}{2} & -\frac{1}{2} \\ 0 & -\frac{\sqrt{3}}{2} & \frac{\sqrt{3}}{2} \end{bmatrix} \begin{bmatrix} f_a^s \\ f_b^s \\ f_c^s \end{bmatrix} \quad (6) \\ [2v_a(k) - v_b(k) - v_c(k)] &= r_s [2i_a(k) - i_b(k) - i_c(k)] \\ &\quad + L_q^r \frac{[2i_a(k) - i_b(k) - i_c(k)] - [2i_a(k-1) - i_b(k-1) - i_c(k-1)]}{T_s} \\ [v_c(k) - v_b(k)] &= r_s [i_c(k) - i_b(k)] \\ &\quad + L_d^r \frac{[i_c(k) - i_b(k)] - [i_c(k-1) - i_b(k-1)]}{T_s} \end{aligned} \quad (7)$$

where f represents the voltage or current variable, k means the k^{th} value of data, and T_s is the sampling time of the measurement equipment. Finally, in order to express the relationship between the inductances and current vector, the 3-phase current should be converted to the magnitude and angle of the vector in the rotation reference frame with Park's transformation (8), (9) and (10).

$$\begin{bmatrix} i_q^r \\ i_d^r \end{bmatrix} = \frac{2}{3} \begin{bmatrix} \cos \theta_{er}^s & \cos(\theta_{er}^s - 120^\circ) & \cos(\theta_{er}^s + 120^\circ) \\ \sin \theta_{er}^s & \sin(\theta_{er}^s - 120^\circ) & \sin(\theta_{er}^s + 120^\circ) \end{bmatrix} \begin{bmatrix} i_a^s \\ i_b^s \\ i_c^s \end{bmatrix} \quad (8)$$

$$I_a = \sqrt{(i_q^r)^2 + (i_d^r)^2} \quad (9)$$

$$\beta = -\arctan \left(\frac{i_d^r}{i_q^r} \right) \quad (10)$$

where θ_{er}^s is 0° as assumed before, I_a is the magnitude of current vector, and β is the angle of current vector referred to q-axis. Due to the zero θ_{er}^s , the q- and d-axis currents are varying with time. Thus, the measured q- and d-axis inductances cover the various current vector states. Their saturation phenomena can be reflected by different current magnitude, and their cross-magnetizing effect can be measured by the variation of current vector angle.

III. EXPERIMENT DEVICES AND SETUP

As mentioned previously, the main purpose of this paper's method is to measure the d- and q-axis inductances considering the saturation and cross-magnetizing effect, and with relatively normal and low cost laboratory equipments. According to the derivative equations, the ideal 3-phase AC voltage source (or current source) is required. Due to desired relationship of current and inductance, the 3-phase AC current source is preferred. In this paper, however, the voltage source will be applied. In the standstill, there is no back electromotive force (Back-EMF) in each phase. The rated phase current usually can be reached at very low voltage exciting. Therefore, the low voltage range has priority when select the voltage source, in order to increase the precision. In addition, there are current components in the equivalent iron-loss resistances [1], which are not the torque-producing

component and rises as the source frequency increasing. Thus relatively low frequency of the AC source also is suggested.

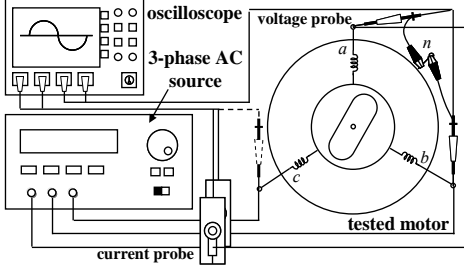


Fig. 1. Experiment setup of inductance measurement applied in this paper

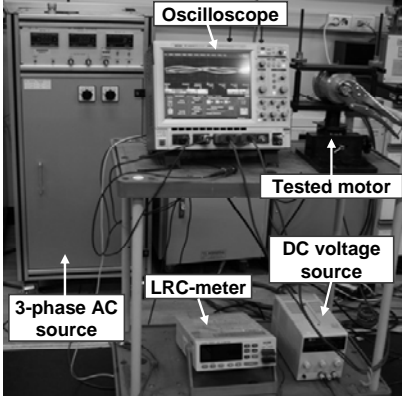


Fig. 3 Experiment setting of inductance measurement

As described in (7), totally there are six variables that should be measured. Unfortunately, more measure channels in oscilloscope implies more expensive price. Due to the asymmetric phase inductance distribution, there is voltage component in the motor neutral line, i.e. the sum of the 3-phase voltages is no longer zero. Meanwhile, the sum of 3-phase currents always equals to zero. Thus, 3-phase voltage and 2-phase current should be measured. In the case of this paper, a 4-channel oscilloscope is applied. One among the 4channels is used to measure the phase c voltage and phase b current, and combine the two groups of measured data in later manufacture. In addition, a DC voltage generator will be helpful to find the rotor zero position. The experiment setup applied in this paper is shown in Fig. 1. The total experiment devices include a 3-phase AC source, a 4-channel oscilloscope, a vice grid pliers, and a DC voltage generator. If the proper 3-phase AC voltage source is unavailable, a 3-phase PM synchronous motor with low total harmonic distortion (THD) Back-EMF could be used to generate the nearly ideal 3-phase voltage. In the case of large Back-EMF, the rheostat can be used to reduce the amplitude of the input voltages. And it is better to use the DC voltage generator to drive the traction DC motor rather than a voltage-chopping controller, in order to generate constant frequency.

IV. EXPERIMENT DATA PROCESSING

A. Tested IPMSM Model and Measurement Device

A 4-pole 6-slot IPMSM is measured in this paper. Its

specifications are listed in Table I. The experiment setting as the realization of Fig. 1 is shown in Fig. 3.

TABLE I
SPECIFICATION OF TESTED MOTOR

Parameter	Value	Unit
Stator outer radii/ Rotor outer radii	79 / 34.5	mm
Airgap length/ Stack length	0.8 / 35	mm
Volume of PM	16×3.5×34	mm ³
Material of core	cogent	
No. of turn in series connected	60	turn
No. of parallel circuits	2	
Phase resistance (@20°C)	0.1593	Ohm
Rated current	9	A _{rms}

B. Experiment Data and Integrating

1) FFT Filter for Smoothing Measured Data

In order to save the data, the digital oscilloscope is used in this paper. The measured voltages and currents hence are discrete-time data. There are much noise in the measured wave forms so that the data cannot be used directly. By means of the FFT filter, the Fourier components whose frequencies are higher than the frequency in (11) can be removed from the original experiment data.

$$f_{threshold} = \frac{1}{n\Delta T} \quad (11)$$

where n is the number of data points considered at one time, and ΔT is the abscissa spacing between two adjacent data points. Fig. 4 shows the comparison between the original data and filtered wave form of phase a voltage.

2) Ripple Elimination

In Fig. 5, it can be seen that the raw inductance results calculated with (7) have serious ripples. The dominate reason is that the slots and poles produces the different permeability in the spatial distribution. Additionally, due to the asymmetric circuit, the variation of current magnitude and vector angle also may generate different saturation and cross-magnetizing effect. In order to eliminate the ripple of calculated inductances, two methods are proposed in this paper. One is that each current point is tested twice. One time makes the rotor align to pole, the other time rotate rotor to align the central of slot. And smooth the wave form by solving the mean value of the calculated inductances in two times. The other method is to use the Polynomial Least-square function to fit the curve. The general k orders polynomial least-square function is described in (12).

$$f(x) = a_0 + a_1x + a_2x^2 + \dots + a_kx^k \quad (12)$$

where $a_0, a_1, a_2, \dots, a_k$ are chosen to minimize the least-square loss function. [7] According to the relationship of current vector angle and electrical position as shown in Fig. 6, the inductance data from 170° to 230° electrical position are chosen and handled. As shown in Fig.5, the ripples in the raw inductance results are totally eliminated. In addition, due to the asymmetric 3-phase currents, the current magnitude varies with electrical position as shown in Fig. 6. The fitted inductances data hence are not about specified current. More testing current points should be measured and make a look-up table about the current magnitude and inductance value for

each desired current vector angle.

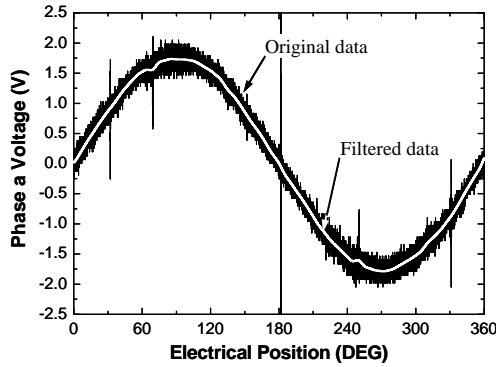


Fig. 4. Comparison between the original data and the filtered data

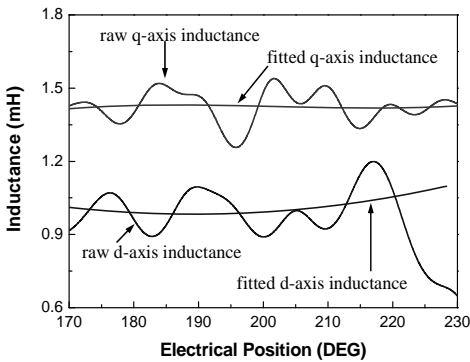


Fig. 5. Comparison between the raw calculated inductances and fitted inductances

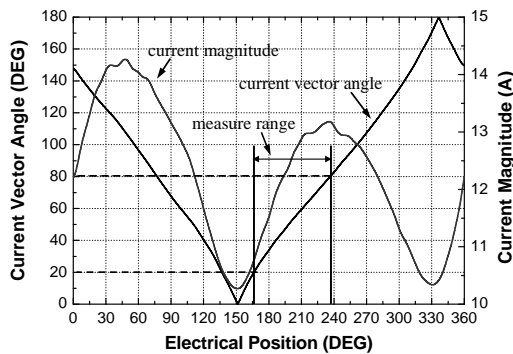
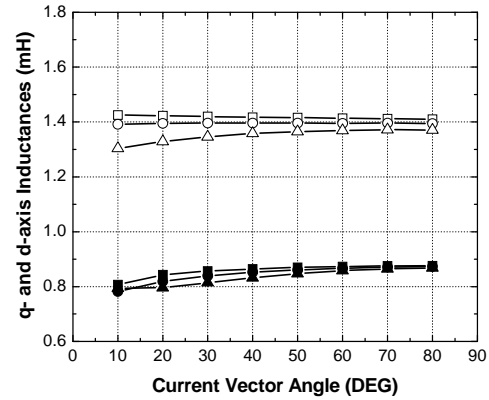


Fig. 6. Variation of current magnitude and vector angle with electrical position

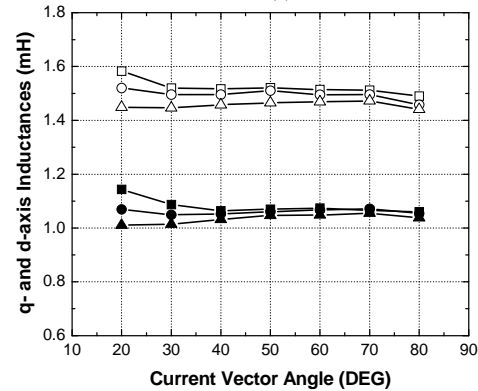
V. RESULT DISCUSSION AND CONCLUSION

The q- and d-axis inductances measured by the proposed method are compared with the numerical analysis results, and shown in Fig. 7. The saturation and cross-magnetizing effect are totally reflected in the results. The numerical inductance calculation method using in this paper, has been introduced and proved in [1]. It can be seen that there is little difference between the measured inductance results and the calculated. Besides the absent leakage inductance in the numerical calculation results, this is mainly because the analysis process does not consider the current components in the iron-loss equivalent resistances. Therefore, larger current is used to produce the flux linkage, the saturation effect becomes more serious.

Due to the sinusoidal current wave form, the denominator



(a)



(b)

Fig. 7. Results comparison: (a) calculated inductances, (b) measured inductances

current terms in (7) may generate the singularity points in the entire electrical period. The measured inductances around these singularity points are strongly distorted, which restricts the measurable inductance range. The current or voltage limitation in the AC source is another drawback of this method, which implies the small power motor is preferred. In the further, more motor will be tested in this proposed method to reveal more advantages and drawback.

REFERENCES

- [1] G. H. Kang, J. P. Hong, etc., "Improved parameter modeling of interior permanent magnet synchronous motor based on finite element analysis," *IEEE Trans. Magn.*, Vol. 36, No. 4, Jul. 2000.
- [2] *IEEE Standard Procedure for Obtaining Synchronous Machine Parameters by Standstill Frequency Response Testing*, IEEE Standard 115A-1987, 1987
- [3] B. Stumberger, G. Stumberger, etc., "Evaluation of saturation and cross-magnetization effects in interior permanent-magnet synchronous motor," *IEEE Trans. Ind. Appl.*, Vol. 39, No. 5, Sept./Oct. 2003.
- [4] E. C. Lovelace, T. M. Jahns, etc., "Design and experimental verification of a direct-drive interior PM synchronous machine using a saturable lumped-parameter model," in *Ind. Appl. Conf.*, Vol. 4, pp. 2486-2492, Oct. 2002.
- [5] K. M. Rahman and S. Hiti, "Identification of machine parameters of a synchronous motor," *IEEE Trans. Ind. Appl.*, Vol. 41, No. 2, Mar./Apr. 2005.
- [6] G.D. Andreescu, etc., "Combined Flux Observer With Signal Injection Enhancement for Wide Speed Range Sensorless Direct Torque Control of IPMSM Drives," *IEEE Trans. Energy Conv.*, vol.23. no. 2, pp.393-402, June. 2008.

- [7] W. H. Press, etc., *Numerical Recipes in C: The Art of Scientific Computing*. Cambridge University Press, Oct. 1992.